A novel one variable first-order shear deformation theory for biaxial buckling of a size-dependent plate based on the Eringen's nonlocal differential law

Mohammad Malikan[1]*, Van Bac Nguyen[2]

[1] Faculty of Engineering, Department of Mechanical Engineering,
Islamic Azad University, Mashhad Branch, Mashhad, Iran

[2] College of Engineering and Technology, Department of Mechanical Engineering
and the Built Environment, University of Derby, Derbyshire, United Kingdom

Abstract

Purpose – This paper presents a new One Variable First-order Shear Deformation Theory (OVFSDT) using nonlocal elasticity concepts for buckling of graphene sheets.

Design/methodology/approach – The FSDT had errors in its assumptions due to assuming constant shear stress distribution along thickness of the plate, even though by using shear correction factor (SCF) it has been slightly corrected, the errors have been remained due to the fact that the exact value of SCF has not already been accurately identified. By utilizing two-variable first-order shear deformation theories these errors decreased further by removing the SCF. In order to consider nanoscale effects on the plate, the Eringen's nonlocal elasticity theory was adopted. The critical buckling loads were computed by Navier's approach. The obtained numerical results were then compared with previous studied results using molecular dynamics simulations and other plate theories for validation which also showed the accuracy and simplicity of the proposed theory. **Findings** – In comparing the biaxial buckling results of the proposed theory with the two-variable shear deformation theories and exact results, it revealed that the two-variable plate theories were not appropriate for the investigation of asymmetrical analyses. **Originality/value** – A formulation for FSDT was innovated by reconsidering its errors in order to improve the FSDT for investigation of mechanical behavior of nanoplates.

Keywords One variable FSDT, nonlocal elasticity theory, graphene sheets

Paper type Research paper

1. Introduction

Graphene sheets have closely-knit carbon atoms that they can work like super-fine atomic nets and also are as an exciting replacement for existing materials that have been pushed to their physical limits. It could revolutionize other areas of technology constrained by conventional materials. For example, it could spawn lighter and stronger airplanes (by replacing composite materials or metal alloys in many structural parts), cost-competitive and more efficient solar panels (replacing silicon again), more energy-efficient power transmission equipment (in place of superconductors), and supercapacitors with thinner plates that can be charged in seconds and store more energy in a smaller space than has ever previously been possible (replacing ordinary, chemical batteries entirely) (Warner *et al.*, 2012; Pati *et al.* 2011). Buckling in plates is one of the most important phenomena in solid mechanics. Thus, theoretical buckling analysis of nanoscale plates has been extensively investigated by researchers around the world to get insight into the mechanical behavior and help characterize

Mohammad Malikan, Van Bac Nguyen

the material properties and also in many cases, to overcome the difficulties encountered in experimental testing and characterization. In order to study of nanoscale's mechanical behavior, there were some size-dependent theories such as modified couple stress theory (Akgöz and Civalek, 2012), strain gradient theory (Hosseini-Hashemi *et al.,* 2017) and Eringen's nonlocal elasticity theory (Golmakani and Rezatalab, 2015). All the mentioned theories could be used for studying the mechanical behavior of nanomaterials. In addition, it is clear that the nonlocal elasticity theory for buckling of nanoplates has been investigated more than other theories for the buckling phenomena (uniaxial, biaxial, shear, thermal and electrical and also a combination of them) (Golmakani and Rezatalab, 2015; Radić and Jeremić, 2016; Ebrahimi and Barati, 2016; Mohammadi *et al.,* 2014). The Eringen's nonlocal elasticity theory has been considered as one of the most useful tools in treating phenomena, whose origins lie in the regimes smaller than the classical continuum models. This theory takes into account of the remote action forces between atoms (Gopalakrishnan and Narendar, 2013; Shahsavari and Janghorban, 2017). In classical local elasticity theories, the stress at a material point depends only on the strain at that point, whereas, in nonlocal elasticity theory, the stress at a material point is a function of the strains at all points on the body; therefore using this assumption the behavior of the nanoplates would be modeled more accurately (Shahsavari and Janghorban, 2017; Jung and Han, 2014; Romano and Barretta, 2017; Shahsavari *et al.,* 2017).

Generally, the theoretical research into buckling of graphene sheets has been continuously carried out for the past two decades [14-29]. Many studies on stability of graphene sheets devoted to contractual plate theories, but there have not been many studies on the refined theories. Senjanovic et al. (Senjanovic *et al.,* 2014) studied a new Mindlin plate theory by investigating shear locking-free using the finite element method. They derived shear deflection based on bending deflection by splitting general displacements. In fact, the total deflection and the two slope angles of plate cross-sections were split into their constitutive parts, resulting with decomposition of plate flexure (bending and transverse shear) and in-plane shear, which is analogous to membrane behavior. Malikan et al. (Malikan *et al.,* 2017) studied the buckling of double-layered graphene sheets under shear and thermal loads in which a model of the nanosheet embedded on an elastic matrix using the nonlocal elasticity was proposed. The first-order shear deformation theory for deriving stability equations and the differential quadrature method were used in order to solve the governing equations. Golmakani and Sadraee Far (Golmakani and Sadraee Far, 2017) investigated the buckling of double-layered nanoplates under biaxial loads in which the nanoplates were embedded on an elastic matrix using differential quadrature method in various boundary conditions. Malikan (Malikan, 2017a) investigated the shear resistance of a piezoelectric nanoplate using a modified couple stress theory which was based on a simple first-order shear deformation theory. The results showed that using this modified couple stress theory led to more accurate results in comparison with other theories. Recently, buckling of graphene sheets subjected to biaxial nonuniform compression using an analytical approach based on a four-variable plate theory was presented in

(Malikan, 2017b). Rezaei et al. (Rezaei *et al.,* 2017) studied a simple four-variable plate theory for considering the natural frequencies of functionally graded plates with porosities. The two decoupled equations were solved analytically for Lévy-type boundary conditions to obtain the Eigen frequencies of the plate. Zenkour et al. (Zenkour *et al.,* 2017) recently proposed a two variable simplified higher-order theory for free vibration behavior of laminated plates. A closed-form solution via Navier's technique limits the applicability of solution technique to simply-supported rectangular laminated plates. The presented plate theory has been considered as an accurate and simple theory that treated the free vibration analysis of moderately thick isotropic, orthotropic and laminated composite plates. Vibration and buckling of orthotropic double-layered graphene sheets under hygrothermal loading with different boundary conditions have been analyzed by Radic and Jeremic (Radić and Jeremić, 2017). Li et al. (Li *et al.,* 2017) proposed a spectral element model for thermal effects on vibration and buckling of laminated beams based on a trigonometric shear deformation theory. Singh and Singh (Singh and Singh, 2017) investigated new higher-order shear deformation theories for free vibration and buckling analysis of laminated and braided composite plates. Two new displacement models Trigonometric Deformation Theory (TDT) and Trigonometric-Hyperbolic Deformation Theory (THDT) were proposed and implemented for free vibration and buckling analysis of laminated and 3D braided composite plates to ensure the efficacy of the analysis. The buckling responses of TDT and THDT were compared with other higher-order theories and showed the applicability of the models for predicting the stability resistance more efficiently for laminated as well as 3D braided composite plates. Navayi Neya et al. (Navayi Neya *et al.,* 2017) analyzed a benchmark solution for buckling of thick rectangular transversely isotropic plates under biaxial load, in which the displacement potential function for deriving governing equations and an analytical solution were presented. Their results showed that the presence of a compressive load along the second axis decreased the buckling load in the plates, and in general, buckling mode, and vice versa. Gupta et al. (Gupta *et al.,* 2017) studied effects of the thermal environment on free vibration and buckling of partially cracked isotropic and functionally graded microplates based on a nonclassical Kirchhoff's plate theory. Results obtained from modified couple stress theory were compared with those obtained from classical plate theory for presence and absence of thermal environment. The results for fundamental frequency obtained from modified couple stress theory were higher for both presence and absence of thermal environment showing the significance of internal material length scale parameter for very thin plates. Thermal buckling and post-buckling analysis of functionally graded beams based on a general higher-order shear deformation theory have been evaluated by Ren et al. (Ren *et al.,* 2017). The results showed that the thermal post-buckling equilibrium paths for FGM beams were stable; also, the critical buckling temperature and the thermal post-buckling strength for Euler-Bernoulli beam model was higher. An analytical solution for buckling of Mindlin plates subjected to arbitrary boundary conditions has been proposed by Ruocco et al. (Ruocco *et al.,* 2017). The model was based on the extended Kantorovich

Mohammad Malikan, Van Bac Nguyen

method and performed a decoupling of variables with respect to two orthogonal coordinate directions. Shahsavari et al. (Shahsavari *et al.,* 2018b) reported different nonlocal strain gradient theories for shear buckling of single-layer graphene sheets in hygrothermal environment resting on an elastic foundation. Khaniki et al. (Khaniki *et al.,* 2017) investigated buckling analysis of nonuniform nonlocal strain gradient beams by using generalized differential quadrature method. The results revealed that when increasing the strain gradient term the required in-plane load for reaching the critical buckling reaction increased; however, while increasing the nonlocal term the required in-plane load decreased.

In general, sheets classified into three groups: thin plates (with small and large deflections), moderately thick and thick plates (Ugural, 1981; Timoshenko and Woinowsky-Kreiger, 1959). The approximate theories of thin plates become unreliable for the case of plates that have considerable moderately thicknesses, especially for the case of highly concentrated loads. In such cases, the moderately thick-plate theory should be applied. This theory considers the problem of plates as a two-dimensional of elasticity. It deems that there is lack of studies on the buckling analysis of graphene sheets by a one variable shear deformation theory of elasticity. This means that there has been so far only one stability equation in terms of the displacement's field for obtaining critical buckling load in such plates. Therefore, an investigation on obtaining stability equations expressed in terms of displacements and rotations, using a combination of FSDT and nonlocal elasticity theories is important in order to accurately gain mechanical behavior of nanoplates. This paper presents a novel formulation for buckling of rectangular single-layered graphene sheet which is resting on Winkler-Pasternak foundation. Governing equations were derived based on a new first-order shear deformation theory and Eringen's nonlocal elasticity theory considering von Kármán strain field. The stability equation was derived in terms of displacements and rotations. In order to achieve numerical results, Navier's solution was taken into account. In order to assess the performances of the proposed theory, the critical buckling loads computed from the proposed theory are compared with those obtained by other theories. Also, a parametric study is performed to demonstrate the behavior of nanoplates on elastic foundations with variable plate dimensions and boundary conditions. Since no simplifying assumption was made in deriving the differential governing equations or in applying the boundary conditions, the method could be applicable for both thin and moderately thick plates.

2. Governing equations

When studying mechanical behavior of nanoplates including buckling, thin plates are usually examined, and the plates should be deployed on an elastic foundation so that the extreme stability conditions are included in the study. In an elastic foundation, both in-plane and transverse resistances could be expressed through shear parameter and stiffness modulus. In addition, a graphene polymer material could be defined as an elastic matrix in static analyses. In this paper, a single-layer graphene sheet (SLGs) resting on an elastic foundation was modeled as a plate embedded in an elastic matrix (Shahsavari *et al.,* 2018a; Shahsavari *et al.,*

2018c; Karami *et al.,* 2018; Malikan and Sadraee Far, 2018). Consider a first-order shear orthotropic rectangular plate of length L_x, width L_y and uniform thickness h, with its middle surface in a Cartesian coordinate system as shown in Figures 1, 2 and 3.

The development of nanotechnologies extends the field of application of the classical or non-classical theories of plates towards the new thin-walled structures (Altenbach and Eremeyev, 2015). Recently, many theories for nanosize plates have been considered and consequently various new theories have been formulated. The classical plate theory (CPT) is inconsistent for thin plates in the sense that elements are assumed to remain perpendicular to the mid-plane, yet equilibrium requires that stress components σ_{xz}, σ_{yz} still arise (which would cause these elements to deform). The theory of moderately thick plates is more consistent, but it still makes the assumption that the stress component $\sigma_z=0$. Note that both are approximations of the three-dimensional elasticity theory (Kelly, 2013). Furthermore, the accurate results for moderately thick plates can be obtained by taking into account the effect of transverse shear deformation and the according theory used is called First-order Shear Deformation Theory (FSDT) or Mindlin's theory. According to FSDT, the following displacement field can be expressed as follows (Malikan and Sadraee Far, 2018):

$$U(x,y,z) = z\,\varphi(x,y) \tag{1a}$$

$$V(x,y,z) = z\,\psi(x,y) \tag{1b}$$

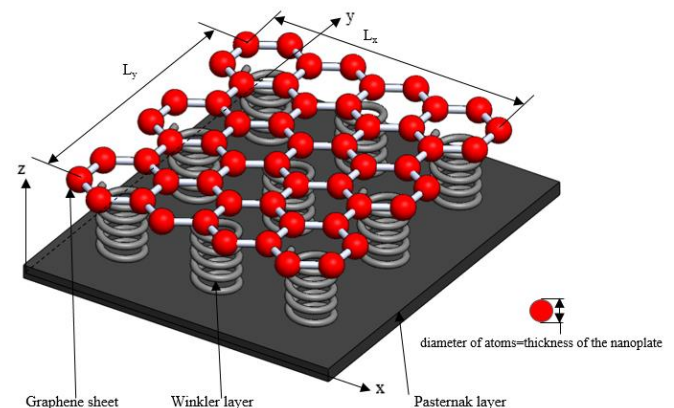$$W(x,y,z) = w(x,y) \tag{1c}$$

Figure 1 Schematic presentation of graphene sheet on an elastic matrix in right-hand coordinate system

where w is the transverse deflection. For the consideration of the transverse shear deformation, the components of the rotation can be written in terms of two functions φ and ψ (Malikan *et al.,* 2017). In vector analysis, the standard procedure of expressing the rotation vector as the sum of the gradient of the scalar φ and the curl of a vector with the z-component ψ was used. In the theory, the shear stress in the thickness direction was given a constant value, which in fact could not be true (Malikan, 2017a). For solving the problem, a shear correction factor (SCF) had to be used, which for various materials could not be exactly defined; therefore a value of 0.833 being often used for various conditions

Mohammad Malikan, Van Bac Nguyen

in previous studies might not be accurate. This is because the value was derived for an isotropic rectangular laminated macro plate only (Madabhusi-Raman and Davalos, 1996) and has not been determined for micro and nanoplates. Therefore, by deriving a simple First-order Shear Deformation Theory (SFSDT), the SCF was removed from governing equations, and the problem has been solved by splitting (w) into the bending component (w_b) and the shear component (w_s) (Malikan, 2017a; Malikan, 2017b; Malikan, 2018a; Malikan, 2018b; Karami and Janghorban, 2016; Karami *et al.,* 2017a; Karami *et al.,* 2017b; Thai and Choi, 2013; Shimpi, 2002):

$$w = w \ (bending) + w \ (shear) \tag{2}$$

Also, the rotation variable in the SFSDT is expressed in terms of the bending component only (Malikan, 2018a):

$$\begin{Bmatrix} \varphi \\ \psi \end{Bmatrix} = \begin{Bmatrix} -\dfrac{\partial w_b}{\partial x} \\ -\dfrac{\partial w_b}{\partial y} \end{Bmatrix} \tag{3a-b}$$

Substituting Eqs. (2, 3) into Eq. (1), the SFSDT displacement field could be written as follows (Malikan, 2018a):

$$\begin{Bmatrix} U(x,y,z) \\ V(x,y,z) \\ W(x,y,z) \end{Bmatrix} = \begin{Bmatrix} -z\dfrac{\partial w_b}{\partial x} \\ -z\dfrac{\partial w_b}{\partial y} \\ w_b(x,y) + w_s(x,y) \end{Bmatrix} \tag{4a-c}$$

The deflection was split into two parameters including shear and bending deflections (Shimpi, 2002). This first study shows that an isotropic square plate was considered for the assumption and as it is vivid, w_s originated from the shear deflection. In fact, for asymmetrical models $\sigma_{xz} \neq \sigma_{yz}$, thus, using a unique variant (w_s) for showing the deflection which resulted from shear stresses in x-z and y-z planes could not be comprehensive for plates with unpredictable behavior and could be conceptual for isotropic square plates and beams only (Figure 2).
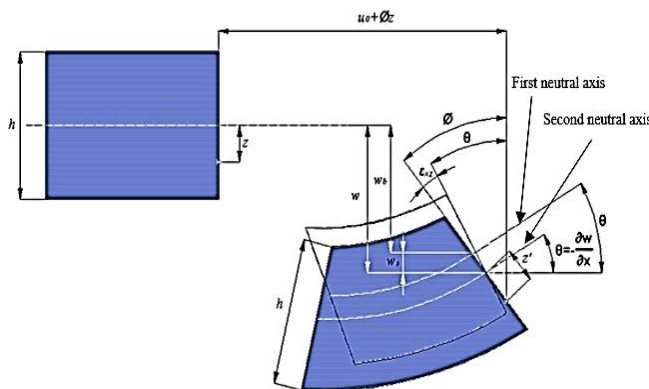

Figure 2 Shear deformation theories presentation (w_s is related to second neutral axis develops from transverse shear stresses taken in FSDT assumptions)

Two states of strain were assumed:
1- The shear strain was derived from the deflection w_s.

2- The deflection w_s was obtained from the shear strain.
For the first state, $w = w_b + w_s$ has been used. However, it should be noted that the second state is the realistic case. Therefore,
$w_{s1} = w_{sx}$, $w_{s2} = w_{sy}$ and $w_{s1} \neq w_{s2}$ because $\varepsilon_{xz} \neq \varepsilon_{yz}$
$w = w_b + w_{s1}$ (or w_{s2})

If $\varepsilon_{xz} > \varepsilon_{yz}$ then w_s occurred due to ε_{xz} thus $w = w_b + w_{s1}$ (5a)

If $\varepsilon_{yz} > \varepsilon_{xz}$ then w_s occurred due to ε_{yz} thus $w = w_b + w_{s2}$ (5b)

These assumptions are applicable for orthotropic, anisotropic, isotropic rectangular plates under asymmetrical loads.

If $\varepsilon_{yz} = \varepsilon_{xz}$ then $w = w_b + w_s$ (6)

This assumption is applicable for isotropic square plates under symmetrical loads and beams.
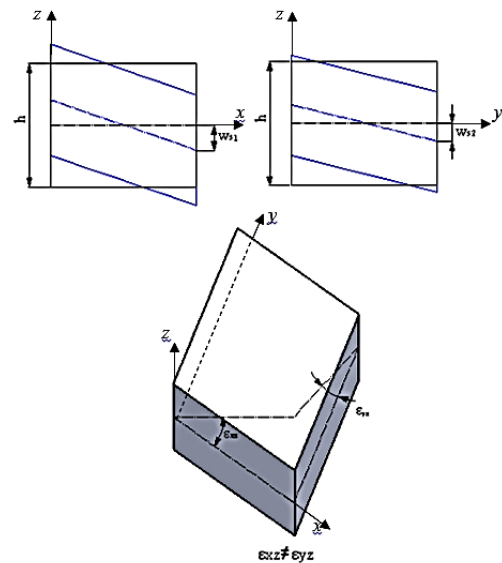

Figure 3 Shear strains in plates

The shear deflection w_s resulted from shear stresses in x-z and y-z planes when Eq. 5 was used, as shown in Figure 3. However, it could not be specified that the value of w_s in the response was still related to x-z or y-z axis planes. Although the w_s could be a unique value for plates which led to close results in comparison with other theories, it was not clear which from axis the value was obtained. The error would be significant when anisotropic and orthotropic plates were considered due to the fact that the response outcomes were considered only by stiffness matrix without variants. To justify these assumptions, let consider other studies in which shear deflection was used as a unique value as shown in Eq. 7-10.

    A) According to (Shimpi, 2002):
RPT :

$$\begin{Bmatrix} U(x,y,z) \\ V(x,y,z) \\ W(x,y,z) \end{Bmatrix} = \begin{Bmatrix} -z\dfrac{\partial w_b(x,y)}{\partial x} + h\left[\dfrac{1}{4}\left(\dfrac{z}{h}\right) - \dfrac{5}{3}\left(\dfrac{z}{h}\right)^3\right]\dfrac{\partial w_s(x,y)}{\partial x} \\ -z\dfrac{\partial w_b(x,y)}{\partial y} + h\left[\dfrac{1}{4}\left(\dfrac{z}{h}\right) - \dfrac{5}{3}\left(\dfrac{z}{h}\right)^3\right]\dfrac{\partial w_s(x,y)}{\partial y} \\ w_b(x,y) + w_s(x,y) \end{Bmatrix}$$

; Excludes shear correction factor

Mohammad Malikan, Van Bac Nguyen

(7a-c)

B) According to (Shimpi et al., 2007):

$NFSDT - I (SFSDT)$:

$$\begin{Bmatrix} U(x,y,z) \\ V(x,y,z) \\ W(x,y,z) \end{Bmatrix} = \begin{Bmatrix} -z \dfrac{\partial w_b(x,y)}{\partial x} \\ -z \dfrac{\partial w_b(x,y)}{\partial y} \\ w_b(x,y) + w_s(x,y) \end{Bmatrix}$$

(8a-c)

; Excludes shear correction factor

C) According to (Shimpi et al., 2007):

$$NFSDT - II : \begin{Bmatrix} U(x,y,z) \\ V(x,y,z) \\ W(x,y,z) \end{Bmatrix} = \begin{Bmatrix} -z \dfrac{\partial \Phi(x,y)}{\partial x} \\ -z \dfrac{\partial \Phi(x,y)}{\partial y} \\ w(x,y) \end{Bmatrix}$$

(9a-c)

; Includes shear correction factor

D) According to (Timoshenko and Woinowsky-Kreiger, 1959):

$$CPT : \begin{Bmatrix} U(x,y,z) \\ V(x,y,z) \\ W(x,y,z) \end{Bmatrix} = \begin{Bmatrix} -z \dfrac{\partial w(x,y)}{\partial x} \\ -z \dfrac{\partial w(x,y)}{\partial y} \\ w(x,y) \end{Bmatrix}$$

(10a-c)

; Thin plates

The comparison of various nondimensional parameters for simply-supported isotropic square plates under sinusoidal transverse loads were shown in Table I whilst the comparison of various nondimensional parameters for simply-supported isotropic square plates under uniformly distributed transverse loads were illustrated in Table II.

Table I Comparison of various nondimensional parameters of simply-supported **isotropic** square plate ($L_y/L_x=1$, $h/L_x=0.1$) under **sinusoidal** transverse load: $\hat{w}=wE/hq_0$, at $x=L_x/2$, $y=L_y/2$, $E_2=E_1=E$, $G_{12}=G_{13}=G_{23}=G=E/2(1+v)$, $v=0.3$.

RPT (Shimpi, 2002)	Exact (Shimpi, 2002)	CPT (Shimpi, 2002)	NFSDT-I and II (Shimpi et al., 2007)
296.0568	294.2375	280.2613	296.0674

Table II Comparison of various nondimensional parameters of simply-supported **isotropic** square plate ($L_y/L_x=1$) under **uniformly** distributed transverse load: $\hat{w}=wG/hq_0$, at $x=L_x/2$, $y=L_y/2$, $E_2=E_1=E$, $G_{12}=G_{13}=G_{23}=G=E/2(1+v)$, $v=0.3$.

h/L_x	Reissner* (Srinivas, 1970)	Exact 3D (Srinivas, 1970)	CPT (Srinivas, 1970)	NFSDT-I and II (Shimpi et al., 2007)
0.05	2760.00	2761.3	2729.9	2765.27
0.1	178.13	178.45	170.62	179.46
0.14	48.247	48.40	44.414	48.92

* The formulation is accessible in (REISSNER, 1945). Reissner plate theory was derived from the variational principle of the complementary strain energy with the assumption of a linear bending stress distribution and a parabolic shear stress distribution. The formulation of the Reissner plate theory will inevitably lead to the displacement variation being not necessarily linear along the plate thickness and also the deformation of the plate thickness (Wang et al., 2001).

Table II clearly demonstrated that the RPT and NFSDT-I had some difference to the exact results when sinusoidal transverse loads were asymmetrical. The comparison of the parameters for simply-supported an isotropic square plate under uniformly load strongly in Table II indicated the shortcoming of RPT and NFSDT-I in comparison with those for asymmetrical analysis in Table I. In addition, it clearly showed that the difference between the results of h/L_x=0.1 in Table I is more than those in Table II. Table III illustrated another comparison for various nondimensional parameters of simply-supported orthotropic square plates under uniformly transverse loading.

Table III Comparison of various nondimensional parameters of simply-supported **orthotropic** square plate (Ly/Lx=1) under **uniformly** distributed transverse load: $\hat{w}=wQ_{11}/hq_0$, at $x=L_x/2$, $y=L_y/2$, $E_2/E_1=0.5225$, $G_{12}=E_1=0.29281$, $G_{13}=E_1=0.17809$, $G_{23}=E_1=0.29713$, $v_{12}=0.44046$, $v_{23}=0.23124$.

h/L_x	Reissner (Srinivas and Rao, 1970)	Exact 3D (Srinivas and Rao, 1970)	CPT (Srinivas and Rao, 1970)	NFSDT-I and II (Srinivas and Rao, 1970)
0.05	10442	10443	10246	10413.4
0.1	688.37	688.57	640.39	681.75
0.14	191.02	191.07	166.7	187.77

The large differences between the results of NFSDT-I and exact theories shown in Table III in comparison with those in Tables I-II were observed and that confirms the significant error of w_s for orthotropic, and generally for asymmetric materials. Although the NFSDT-I value was more accurate than CPT's, it still showed some difference between the NFSDT-I and exact results and also in comparison with Reissner's; this could justify the error existing when using w_s in developing equations. Lastly, if orthotropic rectangular plates under sinusoidal loading were considered, the error would be the largest.

According to the results shown in Tables I - III, the use of $w = w_b + w_s$ was accompanied with the error in the response of the analysis of asymmetrical plates. Furthermore, considering Eq. 5 for deriving displacement field could have difficulties and resulting in complicated mathematical relationships. Therefore, a simple formulation could be developed by removing the *direct effect* of w_s and refining further the SFSDT (NFSDT-I) as shown in the following equations:

Mohammad Malikan, Van Bac Nguyen

$$\begin{Bmatrix} U(x,y,z) \\ V(x,y,z) \\ W(x,y,z) \end{Bmatrix} = \begin{Bmatrix} -z \dfrac{\partial w_b}{\partial x} \\ -z \dfrac{\partial w_b}{\partial y} \\ w_b(x,y) + W' \end{Bmatrix} \quad (11\text{a-c})$$

In which W' is an indirect impact of shear deflection which will be determined.

The best conception way in order to examine the influences of the shear deflection should be examining the bending deflection (w_b) when it was equal in both x-z and y-z planes. In fact, it was the deflection of the second neutral axis (according to Figure 2, we have seen two neutral axes; first about deflection of classical plate theory (CPT) and second related to SFSDT). Therefore, it could be used for finding the value of w_s. Here, by using nonlinear strains of Lagrangian and substituting them into Eq. 4, the strain field of SFSDT was obtained as follows:

$$\begin{cases} \varepsilon_{xx} = -z \dfrac{\partial^2 w_b}{\partial x^2} + \dfrac{1}{2}\left(\dfrac{\partial w_b}{\partial x}\right)^2 + \dfrac{1}{2}\left(\dfrac{\partial w_s}{\partial x}\right)^2 + \dfrac{\partial w_b}{\partial x}\dfrac{\partial w_s}{\partial x} \\[2ex] \varepsilon_{yy} = -z \dfrac{\partial^2 w_b}{\partial y^2} + \dfrac{1}{2}\left(\dfrac{\partial w_b}{\partial y}\right)^2 + \dfrac{1}{2}\left(\dfrac{\partial w_s}{\partial y}\right)^2 + \dfrac{\partial w_b}{\partial y}\dfrac{\partial w_s}{\partial y} \\[2ex] \gamma_{yz} = \dfrac{\partial w_s}{\partial y} \\[2ex] \gamma_{xz} = \dfrac{\partial w_s}{\partial x} \\[2ex] \gamma_{xy} = -2z \dfrac{\partial^2 w_b}{\partial x \partial y} + \left(\dfrac{\partial w_b}{\partial x} + \dfrac{\partial w_s}{\partial x}\right)\left(\dfrac{\partial w_b}{\partial y} + \dfrac{\partial w_s}{\partial y}\right) \end{cases} \quad (12\text{a-e})$$

By substituting Eq. 12 into Hook's law, the stress field can be calculated as follows:

$$\begin{Bmatrix} \sigma_{xx} \\ \sigma_{yy} \\ \sigma_{yz} \\ \sigma_{xz} \\ \sigma_{xy} \end{Bmatrix} = \left[Q_{ijk}\right] \begin{Bmatrix} \varepsilon_{xx} \\ \varepsilon_{yy} \\ \gamma_{yz} \\ \gamma_{xz} \\ \gamma_{xy} \end{Bmatrix} \quad (13\text{a-e})$$

In which Q_{ijk} is the stiffness matrix for the material. The SFSDT stress resultants were obtained in the following forms (Malikan, 2018a):

$$(N_x, N_y, N_{xy}) = \int_{-h/2}^{h/2} (\sigma_x, \sigma_y, \sigma_{xy}) dz \quad (14\text{a})$$

$$(M_x, M_y, M_{xy}) = \int_{-h/2}^{h/2} (\sigma_x, \sigma_y, \sigma_{xy}) z\, dz \quad (14\text{b})$$

$$(Q_x, Q_y) = \int_{-h/2}^{h/2} (\sigma_{xz}, \sigma_{yz}) dz \quad (14\text{c})$$

Then, by substituting Eq. 13 into Eq. 14 the stress resultants are now achieved as (Malikan, 2018a):

$$\begin{Bmatrix} N_{xx} \\ N_{yy} \\ N_{xy} \\ M_{xx} \\ M_{yy} \\ M_{xy} \\ Q_y \\ Q_x \end{Bmatrix} = \begin{bmatrix} A_{11} & A_{12} & 0 & 0 & 0 & 0 & 0 & 0 \\ A_{21} & A_{22} & 0 & 0 & 0 & 0 & 0 & 0 \\ 0 & 0 & A_{66} & 0 & 0 & 0 & 0 & 0 \\ 0 & 0 & 0 & D_{11} & D_{12} & 0 & 0 & 0 \\ 0 & 0 & 0 & D_{21} & D_{22} & 0 & 0 & 0 \\ 0 & 0 & 0 & 0 & 0 & D_{66} & 0 & 0 \\ 0 & 0 & 0 & 0 & 0 & 0 & H_{44} & 0 \\ 0 & 0 & 0 & 0 & 0 & 0 & 0 & H_{44} \end{bmatrix} \times$$

$$\begin{Bmatrix} \dfrac{1}{2}\left(\dfrac{\partial w_b}{\partial x}\right)^2 + \dfrac{1}{2}\left(\dfrac{\partial w_s}{\partial x}\right)^2 + \dfrac{\partial w_b}{\partial x}\dfrac{\partial w_s}{\partial x} \\[2ex] \dfrac{1}{2}\left(\dfrac{\partial w_b}{\partial y}\right)^2 + \dfrac{1}{2}\left(\dfrac{\partial w_s}{\partial y}\right)^2 + \dfrac{\partial w_b}{\partial y}\dfrac{\partial w_s}{\partial y} \\[2ex] \left(\dfrac{\partial w_b}{\partial x} + \dfrac{\partial w_s}{\partial x}\right)\left(\dfrac{\partial w_b}{\partial y} + \dfrac{\partial w_s}{\partial y}\right) \\[2ex] \dfrac{\partial^2 w_b}{\partial x^2} \\[2ex] \dfrac{\partial^2 w_b}{\partial y^2} \\[2ex] \dfrac{\partial^2 w_b}{\partial x \partial y} \\[2ex] \dfrac{\partial w_s}{\partial y} \\[2ex] \dfrac{\partial w_s}{\partial x} \end{Bmatrix} \quad (15\text{a-h})$$

In which constants A_{ij}, D_{ij} ($i, j = 1, 2,$ and 6) and H_{44} were given by (Malikan *et al.*, 2017):

$$H_{44} = G_{12}h \quad (\text{supposed: } G_{12} \cong G_{13} \cong G_{23})$$

$$Q_{11} = \dfrac{E_1}{1 - \upsilon_{12}\upsilon_{21}} = Q_{22}, \; Q_{12} = \dfrac{\upsilon_{12}E_2}{1 - \upsilon_{12}\upsilon_{21}}, \; Q_{66} = G_{12}$$

$$A_{ij}, D_{ij} = \int_{-\frac{h}{2}}^{\frac{h}{2}} \left(1, z^2\right) Q_{ij} dz \quad (i = 1, 2, 6) \quad (16\text{a-f})$$

where E_1 and E_2 are Young's modules, v_{12} and v_{21} denote Poisson's ratios, G_{12} exhibits the shear modulus and h is the thickness of the orthotropic plate. D_{ij} and A_{ij} are the bending and tensioning stiffness matrixes (Malikan *et al.*, 2017).

Here, the fourth equation of FSDT's governing equations (Malikan and Sadraee Far, 2018) was adopted since it was simple to calculate w_s (based on w_b):

$$\dfrac{\partial M_x}{\partial x} + \dfrac{\partial M_{xy}}{\partial y} - Q_x = 0 \quad (17)$$

Now by substituting Eq. 15 into Eq. 17:

$$D_{11} \dfrac{\partial^3 w_b}{\partial x^3} + (D_{12} + D_{66}) \dfrac{\partial^3 w_b}{\partial x \partial y^2} - H_{44} \dfrac{\partial w_s}{\partial x} = 0 \quad (18)$$

By integrating from Eq. 18 with respect to x, simplifying and also ignoring the integral constant, the shear deflection could be obtained as follows:

Mohammad Malikan, Van Bac Nguyen

$$W' = A \frac{\partial^2 w_b}{\partial x^2} + B \frac{\partial^2 w_b}{\partial y^2} \qquad (19)$$

In which, terms A and B are expressed as follows:

$$A = \frac{D_{11}}{H_{44}}, \quad B = \frac{D_{12} + D_{66}}{H_{44}} \qquad (20\text{a-b})$$

Afterwards, the OVFSDT could be achieved in the following equations:

$$\begin{Bmatrix} U(x,y,z) \\ V(x,y,z) \\ W(x,y,z) \end{Bmatrix} = \begin{Bmatrix} -z \dfrac{\partial w_0(x,y)}{\partial x} \\ -z \dfrac{\partial w_0(x,y)}{\partial y} \\ w_0(x,y) + A \dfrac{\partial^2 w_0(x,y)}{\partial x^2} + B \dfrac{\partial^2 w_0(x,y)}{\partial y^2} \end{Bmatrix}$$

$$; w_b = w_0$$

$$(21\text{a-c})$$

By using the OVFSDT field which was mentioned in Eq. 21, the impact of the shear deflection was embedded in displacement field based on the bending deflection rather than using the SCF or w_s variant. In the next stage, by using Lagrangian strains and implementing the von Kármán strains, the OVFSDT strains were expressed as follows:

$$\begin{cases} \varepsilon_{xx} = -z \dfrac{\partial^2 w_0}{\partial x^2} + \dfrac{1}{2}\left(A \dfrac{\partial^3 w_0}{\partial x^3} + B \dfrac{\partial^3 w_0}{\partial x \partial y^2} + \dfrac{\partial w_0}{\partial x} \right)^2 \\[2mm] \varepsilon_{yy} = -z \dfrac{\partial^2 w_0}{\partial y^2} + \dfrac{1}{2}\left(A \dfrac{\partial^3 w_0}{\partial x^2 \partial y} + B \dfrac{\partial^3 w_0}{\partial y^3} + \dfrac{\partial w_0}{\partial y} \right)^2 \\[2mm] \gamma_{yz} = A \dfrac{\partial^3 w_0}{\partial x^2 \partial y} + B \dfrac{\partial^3 w_0}{\partial y^3} \\[2mm] \gamma_{xz} = A \dfrac{\partial^3 w_0}{\partial x^3} + B \dfrac{\partial^3 w_0}{\partial x \partial y^2} \\[2mm] \gamma_{xy} = -2z \dfrac{\partial^2 w_0}{\partial x \partial y} + \left(A \dfrac{\partial^3 w_0}{\partial x^3} + B \dfrac{\partial^3 w_0}{\partial x \partial y^2} + \dfrac{\partial w_0}{\partial x} \right) \\[2mm] \times \left(A \dfrac{\partial^3 w_0}{\partial x^2 \partial y} + B \dfrac{\partial^3 w_0}{\partial y^3} + \dfrac{\partial w_0}{\partial y} \right) \end{cases} \qquad (22\text{a-e})$$

To obtain the total potential energy (V) of the nanoplate, strain energy (S) was included in the potential energy of external loads (Ω) as follows (Malikan, 2018a):

$$V = S + \Omega \qquad (23)$$

where the strain energy in nonlocal form was obtained as follows:

$$\delta S = \iiint_v \sigma_{ij}^{NL} \, \delta \, \varepsilon_{ij} dV \quad , \; i,j = x,y \qquad (24)$$

where subscript NL and L were used to indicate nonlocal parameters. The potential energy of external loads could be defined as follows (Farajpour et al., 2013):

$$\delta \Omega i = \int_0^{L_y} \int_0^{L_x} \left(k_G \nabla^2 wj - k_w \left(wj + wj^2 \right) + q_{vdW} i + q \right) \delta w dx dy$$

$$, \; i = 1,2,3,...,n \; , \; j = 1$$

$$(25\text{a})$$

$$q_{vdW} k = \sum_{j=1}^{n} Cij \left(wi - wj \right) + \sum_{j=1}^{n} eij \left(wi - wj \right)^3 \;,\;\; k = 1,2,3,...,n$$

$$(25\text{b})$$

Where k_w and k_G denote the Winkler coefficient and Pasternak shear modulus respectively, and the van der Waals interaction bond acting on the kth layers is $qvdW$ (k). In addition, q is the transverse force on the single-layered graphene sheet in bending analysis (Malikan et al., 2017). Using the principle of minimum potential energy ($\delta S + \delta \Omega = 0$), the stability equation (based on the one unknown variable in the nonlocal form in displacement field) was obtained for calculating critical buckling load as follows:

$$\delta w_0 = 0:$$

$$D_{11} \frac{\partial^4 w_0}{\partial x^4} + 2\left(D_{12} + D_{66}\right) \frac{\partial^4 w_0}{\partial x^2 \partial y^2} + D_{22} \frac{\partial^4 w_0}{\partial y^4}$$

$$+ D_{11}\left(A \frac{\partial^6 w_0}{\partial x^6} + B \frac{\partial^6 w_0}{\partial x^4 \partial y^2} \right) + \left(D_{12} + D_{66}\right)$$

$$\left(A \frac{\partial^6 w_0}{\partial x^2 \partial y^4} + B \frac{\partial^6 w_0}{\partial y^6} \right) + \left(D_{11} + D_{12} + D_{66}\right)$$

$$\left(A \frac{\partial^6 w_0}{\partial x^4 \partial y^2} + B \frac{\partial^6 w_0}{\partial x^2 \partial y^4} \right) +$$

$$N_x^{NL}\left(\begin{array}{l} A^2 \dfrac{\partial^6 w_0}{\partial x^6} + B^2 \dfrac{\partial^6 w_0}{\partial x^2 \partial y^4} + \dfrac{\partial^2 w_0}{\partial x^2} + \\[2mm] 2AB \dfrac{\partial^6 w_0}{\partial x^4 \partial y^2} + 2A \dfrac{\partial^4 w_0}{\partial x^4} + 2B \dfrac{\partial^4 w_0}{\partial x^2 \partial y^2} \end{array} \right) +$$

$$N_y^{NL}\left(\begin{array}{l} A^2 \dfrac{\partial^6 w_0}{\partial x^4 \partial y^2} + B^2 \dfrac{\partial^6 w_0}{\partial y^6} + \dfrac{\partial^2 w_0}{\partial y^2} + \\[2mm] 2AB \dfrac{\partial^6 w_0}{\partial x^2 \partial y^4} + 2A \dfrac{\partial^4 w_0}{\partial x^2 \partial y^2} + 2B \dfrac{\partial^4 w_0}{\partial y^4} \end{array} \right) +$$

$$k_G \nabla^2 w_0 - k_w w_0 = 0$$

$$(26)$$

In which w_0 is the transverse deflection of the plate, N_x^{NL} and N_y^{NL} are the nonlocal in-plane stress resultants.

The main purpose of the Eringen's differential law was to develop a basic equation to model the nanostructures in a nonlocal continuum model (Eringen, 2002). To this end, the natural extensions of the two fundamental laws of physics to nonlocality included: (i) the energy balance law was postulated to remain in global form; and (ii) a material point of the body was considered to be 'connected' by all points of the body, at all past times (Eringen, 2002). By means of these two natural generalizations of the corresponding local principles, the theory of nonlocal elasticity was formulated (Singh and Singh, 2017). Although the theory was based on linear elasticity and was derived for isotropic materials, it has been adopted in many previous studies for the orthotropic materials and nonlinear behaviors. The local and nonlocal stress-displacement relations were defined as follows (Eringen, 1983; Eringen and Edelen, 1972; Eringen, 2002):

$$\sigma_{ij}(X) = \int_v \lambda_{ijkl}\left(|X' - X|, \alpha\right) \tau_{ij}(X') dV(X') \qquad (27)$$

The above equation could be converted into the following equation (Eringen, 2002):

$$(\zeta + \delta)u_{k,lk} + \mu u_{l,kk} + \left(1 - \mu^2\nabla^2 + \gamma^4\nabla^4\right)\left(\rho f_1 - \rho \ddot{u}_1\right) = 0 \quad (28)$$

Eq. 29 was used rather than classical elasticity that was singularly perturbed. In fact, this equation was used for static problems with vanishing body forces (Eringen, 2002). When the Hookean stress (σ_{kl}) was known, Eq. 29 could be used (Malikan et al., 2017):

$$\left(1 - \mu^2\nabla^2\right)\sigma_{ij}^{NL} = \sigma_{ij}^{L} \quad (29)$$

where σ_{ij}^{NL} is the nonlocal stress and $\mu = (e_0 a)$,

$0 < e_0 a \leq 2nm$ (Golmakani and Rezatalab, 2015) and

also $\nabla^2 = \dfrac{\partial^2}{\partial x^2} + \dfrac{\partial^2}{\partial y^2}$.

There has been no relation for the nonlocal stress resultant; therefore, in order to solve Eq. 26, the stress resultants in the equation had to be in local form by using Eq. 30 as follows (Malikan et al., 2017):

$$\left(1 - \mu^2\nabla^2\right)N_{ij}^{NL} = N_{ij}^{L} \quad (30)$$

By substituting Eq. 30 into Eq. 26 the nonlocal governing equation with local stress resultants Eq. 31 was achieved as follows:

$$D_{11}\frac{\partial^4 w_0}{\partial x^4} + 2\left(D_{12} + D_{66}\right)\frac{\partial^4 w_0}{\partial x^2 \partial y^2} + D_{22}\frac{\partial^4 w_0}{\partial y^4} +$$

$$D_{11}\left(A\frac{\partial^6 w_0}{\partial x^6} + B\frac{\partial^6 w_0}{\partial x^4 \partial y^2}\right) + \left(D_{12} + D_{66}\right)\times$$

$$\left(A\frac{\partial^6 w_0}{\partial x^2 \partial y^4} + B\frac{\partial^6 w_0}{\partial y^6}\right) + \left(D_{11} + D_{12} + D_{66}\right)\times$$

$$\left(A\frac{\partial^6 w_0}{\partial x^4 \partial y^2} + B\frac{\partial^6 w_0}{\partial x^2 \partial y^4}\right) + \left(1 - \mu^2\nabla^2\right)N_x \times$$

$$\left(A^2\frac{\partial^6 w_0}{\partial x^6} + B^2\frac{\partial^6 w_0}{\partial x^2 \partial y^4} + \frac{\partial^2 w_0}{\partial x^2} + 2AB\frac{\partial^6 w_0}{\partial x^4 \partial y^2} \atop +2A\frac{\partial^4 w_0}{\partial x^4} + 2B\frac{\partial^4 w_0}{\partial x^2 \partial y^2}\right) +$$

$$\left(1 - \mu^2\nabla^2\right)N_y \times \left(A^2\frac{\partial^6 w_0}{\partial x^4 \partial y^2} + B^2\frac{\partial^6 w_0}{\partial y^6} + \frac{\partial^2 w_0}{\partial y^2} + \atop 2AB\frac{\partial^6 w_0}{\partial x^2 \partial y^4} + 2A\frac{\partial^4 w_0}{\partial x^2 \partial y^2} + 2B\frac{\partial^4 w_0}{\partial y^4}\right) +$$

$$k_G\left(1 - \mu^2\nabla^2\right)\nabla^2 w_0 - k_w\left(1 - \mu^2\nabla^2\right)w_0 = 0$$

$$(31)$$

Here, the quantities N_x, and N_y are the resultants with respect to the applied in-plane forces ($N_x = k_1 \times N$, $N_y = k_2 \times N$).

3. Solution methodology

The following closed-form solution was obtained for the simple boundary condition of simply-supported plates. Therefore, the general solution for transverse deflection by Navier's method in terms of characteristic modal functions in the following form was adopted (Malikan, 2017b):

$$SSSS; \; w_0 = \sum_{m=1}^{\infty}\sum_{n=1}^{\infty}W_{0mn} \; e^{i\omega t} \sin\left(\lambda x\right)\sin\left(\beta y\right) \quad (32)$$

where $\sin\left(\lambda x\right)$ and $\sin\left(\beta y\right)$ are the characteristic modal functions treated by many researchers satisfying the all sides simply-supported boundary condition, also $\lambda = \dfrac{m\pi}{Lx}$, $\beta = \dfrac{n\pi}{Ly}$, m and n are the half wave numbers, respectively (Malikan, 2017b).

4. Numerical results and discussions

The accuracy of the numerical results originated from the OVFSDT had to be verified by comparing with other theories. In light of the proposed formulation, it was very important to know the difference in the results of the proposed theory and others. Therefore, the results obtained from the proposed theory and validation against those obtained from CPT, FSDT, Exact, and molecular dynamics simulation (MD) theories extracted from well-known references (Golmakani and Rezatalab, 2015; Golmakani and Sadraee Far, 2017; Srinivas, 1970; Ansari and Sahmani, 2013) are presented in Tables IV-VI. It is clearly seen that the results with an increase in the plate's length were becoming closer to the MD's results. Generally, Table IV shows that there was an excellent agreement between the numerical results of the present theory and others', indicating the justification for the proposed theory for square plates in this study. For further validation, Table V presented the comparison between the critical buckling loads obtained by the proposed theory and those of the DQ method (Golmakani and Sadraee Far, 2017) and molecular dynamics simulation (Ansari and Sahmani, 2013) for different aspect ratios of orthotropic single-layered graphene sheets under uniform biaxial compression. The results shows that the new proposed theory had noticeably impacted on the results for rectangular plates. In addition, the variation between results in Table V was more significant than that in Table IV. It should be noted that the MD method was not an exact method, and all the theories presented in the Tables were associated with minor errors because of several reasons; (Golmakani and Rezatalab, 2015; Golmakani and Sadraee Far, 2017) included errors due to approximations used in numerical solutions. On the other hand, MD has some challenges and approximations such as the classical approximation and the interaction potential of atoms (Deuflhard et al., 1999). In fact, the potential is already unknown for materials in many conditions and the proposed potentials have been compared with the experimental test results for being approved. Definitely the proposed potentials could not be exact ones. Another challenge (Ruslan and chack, 2010) in MD for considering a system is to choose an appropriate integration time step. Since this choice is highly system dependent, even the most sophisticated and well developed MD packages leave this choice to the user. In order to make the MD simulation efficient, the step size should be chosen as large as possible. However, too large a step size results in the instability of the numerical integration of the equations of motion. By presenting such an error there is a question that how long

Mohammad Malikan, Van Bac Nguyen

should it runs? This depends on the system and the physical properties of interest (Michael, 2004).

A detailed investigation between the proposed theory and other plate theories is shown in Table VI. Results were provided from the CPT, Mindlin (FSDT) and Exact theories for thin to moderately thick square plates. It can be seen from the Table that the current and Mindlin theories had some differences to the exact theory and these differences increased with increasing the plate thickness. This trend for the OVFSDT was lesser than that of the FSDT. Finally, the OVFSDT was also compared against the SFDT and FSDT in terms of the critical biaxially buckling load for orthotropic plates under in-plane uniform loads and the results are shown in Table VII. It clearly shows that the difference between the OVFSDT's results and the SFSDT's ones for orthotropic behavior was more than those for isotropic behavior, confirming the authors' claim that the SFSDT for asymmetric materials had a minor error. These confirmed that the new theory proposed in this study was able to gain more appropriate and accurate results by carrying out and refining the errors, despite the fact that developing a complete theory was not included in the scope of this study.

Table IV Comparison of critical biaxial buckling loads for single-layered graphene sheet which was simply-supported on all sides from differential quadrature (DQ) method (Golmakani and Rezatalab, 2015; Golmakani and Sadraee Far, 2017), and molecular dynamics simulation (Ansari and Sahmani, 2013). ($E=1TPa$, $v=0.16$, $k_1=1$, $k_2=1$, $k_s=5/6$, $\mu=1.81nm^2$, SSSS).

Critical buckling load (nN/nm)				
OVFSDT	FSDT-DQM (Golmakani and Rezatalab, 2015)	FSDT-DQM (Golmakani and Sadraee Far, 2017)	MD results (Ansari and Sahmani, 2013)	$Lx=Ly$ (nm)
1.0274	1.0749	1.0809	1.0837	4.99
0.62151	0.6523	0.6519	0.6536	8.080
0.43832	0.4356	0.4350	0.4331	10.77
0.26122	0.2645	0.2639	0.2609	14.65
0.17075	0.1751	0.1748	0.1714	18.51
0.11963	0.1239	0.1237	0.1191	22.35
0.08856	0.0917	0.0914	0.0889	26.22
0.06918	0.0707	0.0705	0.0691	30.04
0.05568	0.0561	0.0560	0.0554	33.85
0.04488	0.0453	0.0451	0.0449	37.81

Table V Comparison of critical buckling loads obtained by the proposed theory and those of DQ method (Golmakani and Sadraee Far, 2017) and molecular dynamics (MD) simulation (Ansari and Sahmani, 2013) for different aspect ratios of orthotropic single-layered graphene sheets under uniform biaxial compression. ($E=1TPa$, $v=0.16$, $k1=1$, $k2=1$, $k_s=5/6$, $\mu=1.81nm^2$, SSSS).

Critical buckling load (nN/nm)			
OVFSDT	FSDT-DQM (Golmakani and Sadraee Far, 2017)	MD results (Ansari and Sahmani, 2013)	L_x/L_y
0.52449	0.5115	0.5101	0.5
0.56223	0.5715	0.5693	0.75
0.64225	0.6622	0.6595	1.25
0.75576	0.7773	0.7741	1.5
1.01340	1.0222	1.0183	1.75
1.17030	1.1349	1.1297	2

Table VI Asymptotic λ_x for buckling of orthotropic plates under uniform in-plane force ($k_1=1$, $k_2=0$, $k_s=5/6$, Aragonite crystals, $CaCo_3$ ($E_1=159.958GPa$, $E_2/E_1=0.543103$, $G_{12}/E_1=0.159914$, $G_{13}/E_1=0.17809$, $G_{23}/E_1=0.26681$) (BISPLINGHOFF *et al.*, 1965), SSSS, $\lambda_x = \frac{12}{\pi^2}\frac{P}{E_x}\left(\frac{L_y}{h}\right)^2$).

Dimensionless critical buckling load			
OVFSDT ($E3=0$)	CPT (Srinivas, 1970)	Mindlin* (Srinivas, 1970)	Exact 3D (Srinivas, 1970)	h/L_y
2.9664	3.039	2.965	2.966	0.05
2.7712	3.039	2.768	2.770	0.1
2.2123	3.039	2.204	2.210	0.2

* The formulation was accessible in (MINDLIN, 1951). Mindlin formulated his theory by first assuming a linear variation of displacements along the plate thickness while maintaining the transverse inextensibility of the plate thickness (Wang, 2001). Reviewing the formulation of the plate theories, it is evident that the normal stress σ_{zz} was ignored in the Mindlin plate theory, in contrast to the Reissner plate theory which took into account this normal stress (Wang, 2001).

Table VII The biaxial buckling behavior of orthotropic plates under uniform in-plane loads

($k_1=1$, $k_2=1$, SSSS, Orthotropic graphene sheets: $E_1=1765GPa$, $E_2=1588GPa$, $v_{12}=0.3$, $v_{21}=0.27$, $h=0.34nm$, $L_x=L_y=10.2nm$ (Malikan *et al.*, 2017), $e_0a=0$)

($k_1=1$, $k_2=1$, SSSS, Isotropic graphene sheets: $E=1060GPa$, $v=0.16$, $h=0.34nm$, $L_x=L_y=10.2nm$ (Golmakani and Rezatalab, 2015; Golmakani and Sadraee Far, 2017; Ansari and Sahmani, 2013; He et al., 2005), $e_0a=0$)

Critical buckling load (nN/nm)				
OVFSDT	SFSDT	FSDT ($k_s=5/6$)	FSDT ($k_s=7/8$)	*Mat.*
1.6014	1.5534	1.2943	1.3590	Isotropic
2.3676	2.3081	1.9231	2.0193	Orthotropic

In the parametric investigation, the simply-supported orthotropic nanoplates had the following dimensions and material properties:

Mohammad Malikan, Van Bac Nguyen

$\mu=1.81nm^2$, $Lx=Ly=10.77nm$, $h=0.34nm$, $kw=1.13GPa/nm$, $k_G=1.13Pa.m$, $E_1=1765GPa$, $E_2=1588GPa$, $v_{12}=0.3$, $v_{21}=0.27$ (Malikan *et al.*, 2017)

Figure 4 shows the effects of the small-scale parameter on the square and rectangular orthotropic plates by taking two plate theories. For this purpose, the width of the plate was assumed to be constant and the plate length was given different values. It is clearly seen in Figure 4 that when increasing nonlocal parameter values, i.e. from $\mu=1$ to $\mu=4$ nm^2, critical buckling loads reduced gradually and they got closer for different length ratios. In fact, the impact of different lengths is decreasing with an increase in the nonlocal parameter. Moreover, when the value of plate length increased, the differences between OVFSDT and SFSDT will be larger. As a rule, this is a result of asymmetric plates versus square ones. To another conclude, it can be stated that the increase of nonlocal parameter can reduce the influence of shear stress errors for orthotropic plates.
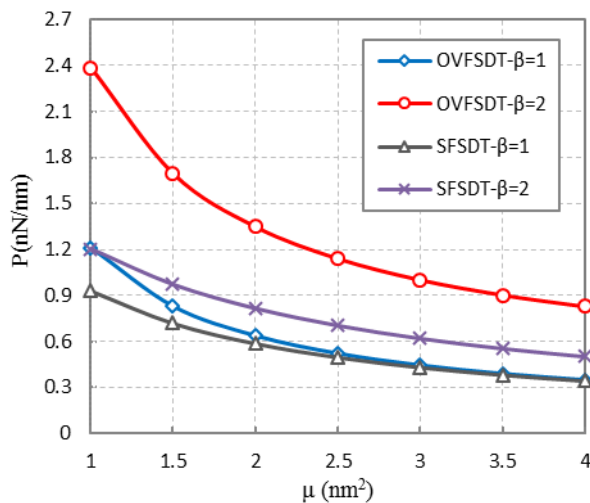

Figure 4 Effect of small-scale parameter on the critical buckling load by considering various aspect ratios ($\beta=Lx/Ly$)

Figure 5 shows the influence of the elastic foundation on the biaxial critical buckling by taking into account several conditions. As can be observed, after embedding the nanoplate on the matrix, the critical buckling load was increasing when the foundation stiffness increased; however, this remarkable increasing trend in the response outcomes was not continued after $kw=1$ GPa/nm. In addition, it is observed that the elastic foundation has further impacted on results of OVFSDT versus SFSDT results while $0 \leq kW \leq 1$ GPa/nm. In plotting the curves in Figure 5, the value of k_G was picked up at 1.13 $Pa.m$.
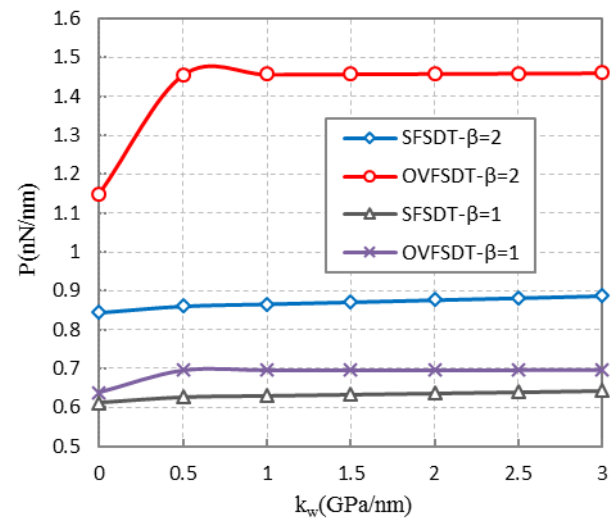

Figure 5 Effect of the elastic foundation versus various aspect ratios on the critical buckling load

Comparison between the results of uniaxial and biaxial critical buckling loads are illustrated in the Figure 6. As expected, regarding asymmetric analysis ($k_1=1$, $k_2=0$), there was a further difference in the results of SFSDT versus OVFSDT in lower values of nanoscale factor. In addition, the critical buckling loads of uniaxial cases were significantly greater than those of biaxial case in same conditions, and the descending slope was also greater in the case of uniaxial analysis. An important consequence could be the closeness of the critical buckling loads for both cases when values of the nonlocal parameter were greater.
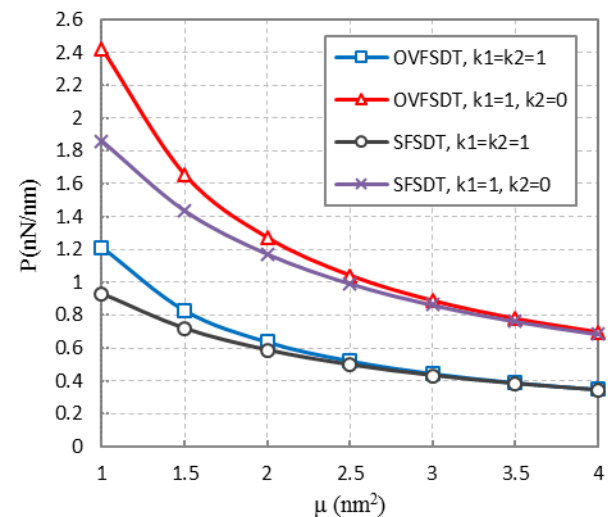

Figure 6 Uniaxial and biaxial critical buckling loads versus small scale parameters

Figure 7 shows the critical buckling loads of thin and moderately thick nanoplates for several different values of the nonlocal parameter (Figure 7a) and for the comparison of results in SFSDT versus OVFSDT (Figure 7b). It can be seen from the Figures that

Mohammad Malikan, Van Bac Nguyen

when the nonlocal parameter increased or when the plate became thicker, the slope of the critical buckling load data increased more dramatically. It is also clear that with an increase in thickness of the plate, the gap between values of the nonlocal parameter for the same dimension ratio (h/L_x) was getting larger. In fact, the small-scale parameter had more impact on thicker plates under stability conditions. By investigation of Figure 7b, it can also be seen that the difference of the diagrams of SFSDT and OVFSDT will increase by increasing thickness which leads to this significant outcome that the effect of a further increase in thickness of the plate shows a simultaneous increase in errors resulted from SFSDT. It also shows that further significant increase in critical buckling loads was observed for plates having greater dimension ratios.
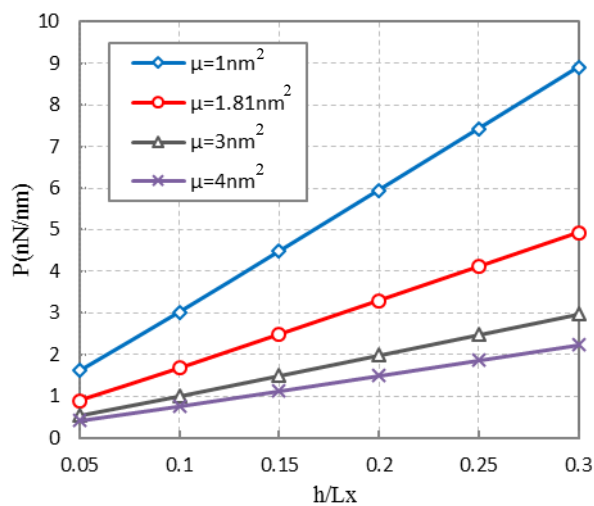

Figure 7a Influences of the ratio of thickness to length versus several small scale parameters on the critical buckling loads
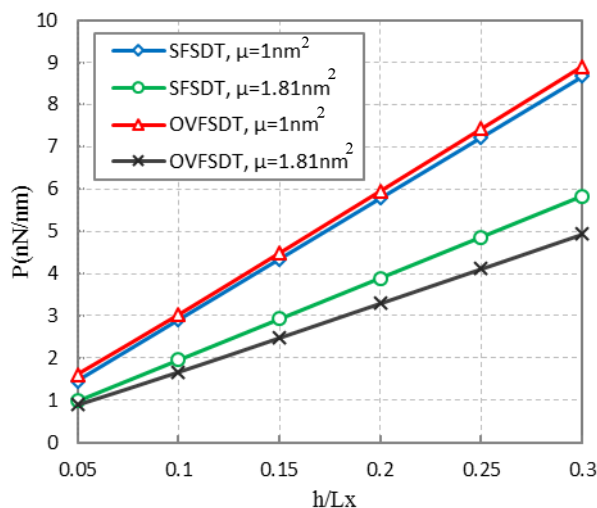

Figure 7b Influences of the ratio of thickness to length on the critical buckling loads for OVFSDT and SFSDT theories

5. Conclusion

The biaxial buckling behavior of the embedded graphene sheet on an elastic foundation was studied using a new One Variable First-order Shear Deformation Theory (OVFSDT). The new OVFSDT theory was developed in reducing the shear deformation error in the buckling responses and the stability equation was determined by applying the nonlocal elasticity theory. The critical buckling load of the orthotropic nanoplates under uniaxial and biaxial loading was successfully computed using the Navier's solution method. The effects of nanoplate′s geometry, different lengths, size-dependent parameter and the elastic foundation on the uniaxial and biaxial buckling responses of the orthotropic nanoplates were examined using the new proposed theory. The validation confirmed that the proposed theory was able to gain more appropriate and accurate results by carrying out and refining the errors in incorporating shear deformation. The proposed theory helped improve the FSDT for investigation of mechanical behavior of nanoplates resting on an elastic foundation and thus, ultimately helped understand the behavior of graphene sheets under stability conditions. In many cases, it would provide an alternative approach to understand and characterize the behavior and material properties of graphene sheets to the experimental tests that are expensive and time consuming. As we know, plates have been used widely in industry as important elements in machines. Many parts which have been made by plates are under stability conditions and it is necessary to know the buckling resistance of the plate to axial loads for designing of the machines parts. Therefore, the theoretical analysis of the nanoplate would help designers to predict the strength of nanosheets or to characterize the nanomaterials used. The theoretical analysis would also help formulate simplest but accurate equations for design practice. According to the numerical results of the present study, the following conclusions are notable.

- The two-variable plate theories (SFSDT, RPT, NFSDT-I) could not be appropriate solutions for asymmetrical analysis.
- When increasing nonlocal parameter values, critical buckling loads reduced gradually and they got closer to each other for different length ratios
- An important consequence could be the closeness of the critical buckling loads in both uniaxial and biaxial cases when values of the nonlocal parameter became greater.
- The small-scale parameter had more impact on the critical buckling load of thicker plates under stability conditions.
- Further increase in critical buckling loads was considerable with an increase in thickness of the plate.
- With increasing nonlocal parameter, results of OVFSDT and SFSDT with noticeable reduction have become closer to each other.

Acknowledgement

References

Akgöz, B., Civalek, Ö. (2012), "Free vibration analysis for single-layered graphene sheets in an elastic matrix via modified couple stress theory", *Materials and Design*, Vol. 42, pp. 164-171.

Altenbach, H., Eremeyev, V. A. (2015), "On the Theories of Plates and Shells at the Nanoscale", *Shell and Membrane Theories in Mechanics and Biology*, Springer, Cham, pp. 25-57. https://doi.org/10.1007/978-3-319-02535-3_2

Ansari, R., Sahmani, S. (2013), "Prediction of biaxial buckling behavior of single-layered graphene sheets based on nonlocal plate models and molecular dynamics simulations", *Applied Mathematical Modelling*, Vol. 37 No. 12-13, pp. 7338–7351.

Bahadur Singh, D., Singh, B. N. (2017), "New higher order shear deformation theories for free vibration and buckling analysis of laminated and braided composite plates", *International Journal of Mechanical Sciences*, Vol. 131–132, pp. 265-277.

Bakhshi Khaniki, H., Hosseini-Hashemi, Sh. and Nezamabadi, A. (2017), "Buckling analysis of nonuniform nonlocal strain gradient beams using generalized differential quadrature method", *Alexandria Engineering Journal*, http://dx.doi.org/10.1016/j.aej.2017.06.001.

BISPLINGHOFF, R. L., MAR, J. W., and PIAN, T. H. H. (1965), "Statics of deformable solids", Chapter 7, Addison-Wesley.

Bouazza, M., Kenouza, Y., Benseddiq, N. and Zenkour, A. M. (2017), "A two-variable simplified nth-higher-order theory for free vibration behavior of laminated plates", *Composite Structures*, Vol. 182, pp. 533-541.

Deuflhard, P., Hermans, J., Leimkuhler, B., Mark, A. E., Reich S. and Skeel, R. D. (1999), "Computational Molecular Dynamics: Challenges, Methods, Ideas", Proceeding of the 2nd International Symposium on Algorithms for Macromolecular Modelling, Berlin, Springer-Verlag Berlin Heidelberg, Vol. 4, DOI: 10.1007/978-3-642-58360-5.

Ebrahimi, F., Barati, M. R. (2016), "Electromechanical buckling behavior of smart piezoelectrically actuated higher-order size-dependent graded nanoscale beams in thermal environment", *International Journal of Smart and Nano Materials*, Vol. 7 No.2, pp. 69-90.

Eringen, A.C. (2002), "Nonlocal Continuum Field Theories", Springer-Verlag, New York.

Eringen, A.C. (1983), "A Nonlocal Finite Element Approach to Nano beams", *Journal of Applied Physics*, Vol. 54, pp. 4703–4710.

Eringen, A.C., Edelen, D. G. B. (1972), "On Nonlocal Elasticity", *International Journal of Engineering Sciences*, Vol. 10, pp. 233–248.

Farajpour, A., Solghar, A. A. and Shahidi, A. (2013), "Postbuckling analysis of multi-layered graphene sheets under non-uniform biaxial compression", *Physica E: Low-dimensional Systems and Nanostructures*, Vol. 47, pp. 197–206.

Golmakani, M. E., Rezatalab, J. (2015), "Nonuniform biaxial buckling of orthotropic Nano plates embedded in an elastic medium based on nonlocal Mindlin plate theory", *Composite Structures*, Vol. 119, pp. 238-250.

Golmakani, M. E., Sadraee Far, M. N. (2017), "Buckling analysis of biaxially compressed double-layered graphene sheets with various boundary conditions based on nonlocal elasticity theory", *Microsystem Technologies*, Vol. 23 No. 6, pp. 2145-2161.

Gopalakrishnan, S., Narendar, S. (2013), "Wave propagation in nanostructures", *Nanoscience and Technology*, Springer, Switzerland.

He, X. Q., Kitipornchai, S. and Liew, K. M. (2005), "Resonance analysis of multi-layered graphene sheets used as nanoscale resonators", *Nanotechnology*, Vol. 16 No. 10, pp. 2086–2091.

Joshi, P. V., Gupta, A., Jain, N. K., Salhotra, R., Rawani, A. M. and Ramtekkar, G. D. (2017), "Effect of thermal environment on free vibration and buckling of partially cracked isotropic and FGM micro plates based on a nonclassical Kirchhoff's plate theory: An analytical approach", *International Journal of Mechanical Sciences*, Vol. 131–132, pp. 155-170.

Jung, W-Y., Han, S-C. (2014), "Nonlocal elasticity theory for transient analysis of higher-order shear deformable nanoscale plates", *Journal of Nanomaterials*, Vol. 2014, 8 pages. http://dx.doi.org/10.1155/2014/208393.

Kelly, P. (2013), "Solid mechanics part II: Chapter 6, Plate theory: Limitations of Classical Plate Theory", *Solid mechanics lecture notes*, University of Auckland.

Karami, B., Janghorban, M. (2016), "Effect of magnetic field on the wave propagation in nanoplates based on strain gradient theory with one parameter and two-variable refined plate theory", *Modern Physics Letters B*, Vol. 30 No. 36, pp. 1650421.

Karami, B., Janghorban and M., Tounsi, A. (2017a), "Effects of triaxial magnetic field on the anisotropic nanoplates", *STEEL AND COMPOSITE STRUCTURES*, Vol. 25 No. 3, pp. 361-374.

Karami, B., Shahsavari, D. and Li Li. (2018a), "Hygrothermal wave propagation in viscoelastic graphene under in-plane magnetic field based on nonlocal strain gradient theory", *Physica E: Low-dimensional Systems and Nanostructures*, Vol. 97, pp. 317–327.

Karami, B., Shahsavari, D., Janghorban, M. and Li Li. (2018), "Wave dispersion of mounted graphene with initial stress", *Thin-Walled Structures*, Vol.122, pp. 102–111.

Karami, B., Shahsavari, D. and Janghorban, M. (2017b), "Wave propagation analysis in functionally graded (FG) nanoplates under in-plane magnetic field based on nonlocal strain gradient theory and four variable refined plate theory", *Mechanics of Advanced Materials and Structures*, https://doi.org/10.1080/15376494.2017.1323143.

Li, J., Jiang L. and Li, X. (2017), "A spectral element model for thermal effect on vibration and buckling of laminated beams based on trigonometric shear deformation theory", *International Journal of Mechanical Sciences*, Vol. 133, pp. 100-111.

Malikan, M., Jabbarzadeh, M. and Dastjerdi, Sh. (2017), "Non-linear Static stability of bi-layer carbon nanosheets resting on an elastic matrix under various types of in-plane shearing loads

in thermo-elasticity using nonlocal continuum", *Microsystem Technologies*, Vol. 23 No. 7, pp. 2973-2991.

Malikan, M. (2017a), "Electro-mechanical shear buckling of piezoelectric nanoplate using modified couple stress theory based on simplified first order shear deformation theory", *Applied Mathematical Modelling*, Vol. 48, pp. 196–207.

Malikan, M. (2017b), "Analytical predictions for the buckling of a nanoplate subjected to nonuniform compression based on the four-variable plate theory", *Journal of Applied and Computational Mechanics*, Vol. 3 No. 3, pp. 218–228.

Malikan, M. (2018a), "Temperature influences on shear stability of a nanosize plate with piezoelectricity effect", *Multidiscipline modeling in materials and structures*, Vol. 14 No. 1, pp. 125-142.

Malikan, M. (2018b), "Buckling analysis of a micro composite plate with nano coating based on the modified couple stress theory", *Journal of Applied and Computational Mechanics*, Vol. 4 No. 1, pp. 1–15.

Malikan, M., Sadraee Far, M. N. (2018), "Differential quadrature method for dynamic buckling of graphene sheet coupled by a viscoelastic medium using neperian frequency based on nonlocal elasticity theory", *Journal of Applied and Computational Mechanics*, Vol. 4 No. 3, pp. 147-160.

Madabhusi-Raman, P., Davalos, J. F. (1996), "Static shear correction factor for laminated rectangular beams", *Composites: Part B*, Vol. 27 No. 3-4, pp. 285-293.

Mohammadi, M., Farajpour, A., Moradi, A. and Ghayour, M. (2014), "Shear buckling of orthotropic rectangular graphene sheet embedded in an elastic medium in thermal environment", *Composites: Part B*, Vol. 56, pp. 629–637.

Moslemi, A., Navayi Neya, B. and Vaseghi Amiri, J. (2017), "Benchmark solution for buckling of thick rectangular transversely isotropic plates under biaxial load", *International Journal of Mechanical Sciences*, Vol. 131–132, pp. 356-367.

Michael, P. A. (2004), "Introduction to molecular dynamics simulation", Computational soft matter: from synthetic polymers to proteins, John von Neumann institute for computing, NIC series, Vol. 23, pp. 1-28.

MINDLIN, R., D. (1951), "Influence of rotary inertia and shear on flexural motions of isotropic elastic plates", *Journal of Applied Mechanics*, Vol. 18 No. 1, pp. 31-38.

Pati, S. K., Enoki, T. and Rao, C. N. R. (2011), "Graphene and Its Fascinating Attributes", *World Scientific Publishing*, Singapore.

Radić, N., Jeremić, D. (2016), "Thermal buckling of double-layered graphene sheets embedded in an elastic medium with various boundary conditions using a nonlocal new first-order shear deformation theory", *Composites Part B*, Vol. 97, pp. 201-215.

Radić, N., Jeremić, A. (2017), "Comprehensive study on vibration and buckling of orthotropic double-layered graphene sheets under hygrothermal loading with different boundary conditions", *Composites part: B*, Vol. 128, pp. 182-199.

REISSNER, E. (1945), "The effect of transverse shear deformation on the bending of elastic plate", *Transactions of the ASME: Journal of Applied Mechanics*, Vol. 12, pp. A69-A77.

Rezaei, A. S., Saidi, A. R., Abrishamdari, M. and Pour Mohammadi, M. H. (2017), "Natural frequencies of functionally graded plates with porosities via a simple four variable plate theory: An analytical approach", *Thin-Walled Structures*, Vol. 120, pp. 366-377.

Romano, G., Barretta, R. (2017), "Nonlocal elasticity in nanobeams: the stress-driven integral model", *International Journal of Engineering Science*, Vol. 115, pp. 14-27.

Ruocco, E., Mallardo, V., Minutolo, V. and Di Giacinto, D. (2017), "Analytical solution for buckling of Mindlin plates subjected to arbitrary boundary conditions", *Applied Mathematical Modelling*, Vol. 50, pp. 497-508.

Ruslan, L., chack, D. (2010), "Discretization errors in molecular dynamics simulations with deterministic and stochastic thermostats", *Journal of Computational Physics*, Vol. 229, pp. 9323-9346.

Senjanovic, I., Vladimir, N. and Hadzic, N. (2014), "Modified Mindlin plate theory and shear locking-free finite element formulation", *Mechanics Research Communications*, Vol. 55, pp. 95– 104.

Shahsavari, D., Janghorban, M. (2017), "Bending and shearing responses for dynamic analysis of single-layer graphene sheets under moving load", *Journal of the Brazilian Society of Mechanical Sciences and Engineering*, Vol. 39 No. 10, pp. 3849-3861.

Shahsavari, D., Karami, B., Janghorban, M. and Li Li. (2017), "Dynamic characteristics of viscoelastic nanoplates under moving load embedded within visco-Pasternak substrate and hygrothermal environment", *Materials Research Express*, Vol. 4 No. 8, pp. 085013.

Shahsavari, D., Karami, B. and Mansouri, S. (2018b), "Shear buckling of single layer graphene sheets in hygrothermal environment resting on elastic foundation based on different nonlocal strain gradient theories", *European Journal of Mechanics - A/Solids*, Vol. 67. pp. 200-214.

Shahsavari, D., Shahsavari, M., Li Li. and Karami, B. (2018c), "A novel quasi-3D hyperbolic theory for free vibration of FG plates with porosities resting on Winkler/Pasternak/Kerr foundation", *Aerospace Science and Technology*, Vol. 72, pp. 134-149.

She, Gui-Lin., Yuan, Fuh-Gwo., and Ren, Yi-Ru. (2017), "Thermal buckling and post-buckling analysis of functionally graded beams based on a general higher-order shear deformation theory", *Applied Mathematical Modelling*, Vol. 47, pp. 340-357.

Shimpi, R. P. (2002), "Refined Plate Theory and Its Variants", *AIAA JOURNAL*, Vol. 40. pp. 137-146.

Shimpi, R. P., Patel, H. G., Arya, H. (2007), "New first order shear deformation theories", *Transactions of the ASME, Journal of Applied Mechanics*, Vol. 74, pp. 523-533.

Srinivas, S., (1970), "Three Dimensional Analysis of Some Plates and Laminates and a Study of Thickness Effects", Ph.D. Dissertation, Dept. of Aeronautical Engineering, Indian Inst. of Science, Bangalore, India.

Srinivas, S., Rao, A. K. (1970), "Bending, Vibration and Buckling of Simply-Supported Thick Orthotropic Rectangular Plates and

Mohammad Malikan, Van Bac Nguyen

Laminates", *International Journal of Solids Structures*, Vol. 6 No. 11, pp. 1463-1481.

Timoshenko, S., Woinowsky-Kreiger, S. (1959), "Theory of plates and shells", Second edition. McGraw Hill, New York.

Thai, H. T., Choi, D. H. (2013), "A simple first-order shear deformation theory for laminated composite plates", *Composites Structures*, Vol. 106, pp. 754–763.

Tohidi, H., Hosseini-Hashemi, S. H. and Maghsoudpour, A. (2017), "Nonlinear size-dependent dynamic buckling analysis of embedded micro cylindrical shells reinforced with agglomerated CNTs using strain gradient theory", *Microsystem Technologies*, Vol. 23 No. 12, pp. 5727–5744.

Ugural, A. C. (1981), "Stresses in plates and shells", ISBN 0-07-065730-0, McGraw Hill Book Company, New York.

Wang, C. M., Lim, G.T., Reddy, J. N. and Lee, K.H. (2001), "Relationships between bending solutions of Reissner and Mindlin plate theories", *Engineering Structures*, Vol. 23, pp. 838–849.

Warner, J. H., Franziska, S., Rummeli. M. and Bachmatiuk, A. (2012), "Graphene: Fundamentals and emergent applications", First edition. ELSEVIER, USA.

Corresponding author

Mohammad Malikan can be contacted at:
mohammad.malikan@yahoo.com